Article

Journal of Vibration and Control
18(13) 2031–2038
© The Author(s) 2011
Reprints and permissions:
sagepub.co.uk/journalsPermissions.nav
DOI: 10.1177/1077546311429340
jvc.sagepub.com

Vibration isolation pad for medical purposes: modeling and simulation

Ahmed Abu Hanieh

Abstract

This project aims at establishing new research about protecting sensitive human beings from vibration syndrome. The main application targeted here is the protection of patients undergoing the Magnetic Resonance Imaging test where noise and vibration can cause severe damage to the test results. Stability and accuracy are very important issues in this medical test. An active vibration isolation pad will be designed and manufactured in this research where the force of the vibrating human body is measured and compensated to be fed back to a linear piezoelectric actuator to isolate the disturbing source of vibrations from propagating into the patient's body. This paper presents analytical and numerical models for the vibration isolation system where the Integral Force Feedback control technique is applied. The results prove high authority and robustness for this control technique especially on the first vibration mode.

Keywords

Finite element model, integral force feedback, magnetic resonance imaging, MRI, piezoelectric actuator, vibration isolation

Received: 28 June 2011; accepted: 3 October 2011

1. Introduction

There are two main components of the Magnetic Resonance Image (MRI) scanner; the large and heavy main magnet and the smaller and lighter gradient coil placed inside the main magnet. The main magnet provides a strong magnetic field (up to several Tesla), while the gradient coil produces a weak magnetic field. The gradient coil is turned on and off very rapidly in a specific manner to alter the main magnetic field at a very local level. Due to the strong main magnetic field, excessive Lorentz forces are produced that act on the gradient coil (Evans, 2003). As a result, the gradient coil vibrates. This produces undesired sound radiation. Indirectly, the forces also cause vibrations in the main magnet housing (receiver) to which the gradient coil (source) is connected. As a consequence, the housing will also emit sound (Evans and Philbin, 2000).

Floor vibration can also cause small magnet displacements that result in distortions or artifacts on the scan image. MRI systems have large, massive magnets that require high strength floors to accommodate the large concentrated floor load. Slab-on-grade floors are inherently better than column-supported or suspended slabs, because they have great bearing capacity and the contact with the sub-floor soil or compacted fill damps the floor slab, so that it exhibits little or no resonant amplification of vibration (Evans, 2004).

Many passive ways have been tested to reduce the impact of vibration on MRI but most of these techniques lead to relatively low damping ratios and insufficient influence. To increase the isolation performance, active techniques can be the best solution. Using active suspension systems for the MRI system itself is costly and difficult. This is because of the very high mass of the system that exceeds 5000 kg where, apart from hydraulics, it is extremely difficult to find actuators that can give this high force. The previous discussion leads to the necessity of finding an isolation system for the patient himself. Besides the fact that such a portable

Birzeit University, Birzeit, Palestinian Territory (occupied)

Corresponding author:
Ahmed Abu Hanieh, Birzeit University, PO Box 14, Birzeit, Palestinian Territory (occupied)
Email: ahanieh@birzeit.edu

isolation pad can be transported with the patient to be used in other medical treatment places (Standlee and Begin, 2003).

Jaensch et al. (2007) discuss a technique to install an MRI around the patient as a part of the pre-polarization system. This technique depends on applying a very large magnetic field in a short period. An experimental test rig has been tested and modeled using Finite Element modeling. The patent shown in Schubert et al. (1994) presents a single-axis two degrees-of-freedom vibration isolation system based on using a stiff mount with a piezoelectric actuator and an intermediate passive soft mount. The control technique used in the patent is different from the one used in this paper. They base their control on summing the signals measured on the velocity of the intermediate mass and the displacement of the quiet payload. Nelson (1991) discusses another similar vibration isolation system but this time it is based on using two soft mounts on top of each other, using a soft voice coil actuator for the purpose of active control. Wakui (2002) came out with a new design of the vibration isolator. In this patent, the author combines between the stiff and soft mounts in a hybrid system where the system uses a stiff piezoelectric actuator in series with another active soft mount using an electromagnetic actuator. The control technique in this system is dependent on using the Proportional + Integral + Derivative (PID) compensator for the two control loops. Le Letty and Claeyssen (1998) present different designs and assemblies of piezoelectric actuators showing their manufacturing procedure and the FEMs. Hao (2008) discusses a passive elastomeric vibration isolation pad designed to reduce the influence of vibrations induced by the hand-held machine tools to avoid Hand Arm Vibration Syndrome (HAVs). Abu Hanieh (2008) depicts an active vibration isolator for the application of vibration isolation to prevent HAVs. The principle discussed here is based on using a stiff piezoelectric actuator with frequency reduction technique using a Proportional plus Integral (PI) controller. Mechefske et al. (2004) contains a wide discussion about the study and characterization of the noise caused by the vibration of the gradient coil in an MRI. This reference shows several experimental results and FEMs. The suggested design in this paper is based on using a stiff mount with a piezoelectric actuator in a series with a soft mount of rubber. This design leads to having a vibration isolator which is able to use the high efforts of piezoelectric actuators (700 Newton) to damp and isolate disturbances at low frequency (3.5 Hz). It is worth mentioning that using the Integral Force Feedback (IFF) control technique leads to softening the structure which reduces the cut-off frequency but this is accompanied with the risk of weakness in carrying the static loads.

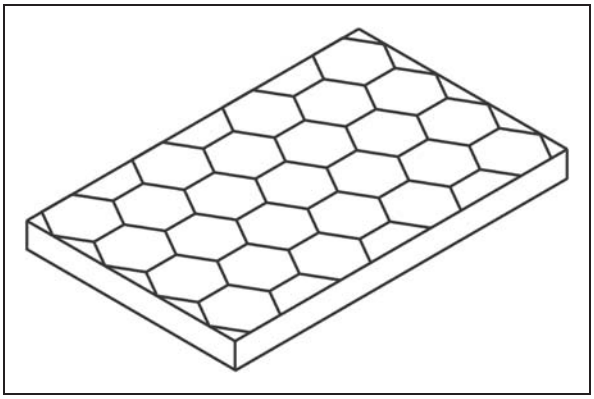

Figure 1. Hexagonal honeycomb configuration of the pad.

The most important difference between this design and other designs shown in the literature is that the effort of vibration isolation is concentrated here on the pad under the patient, which exerts relatively low forces, instead of applying control to the extremely high weight magnets. This fact means that this technique is expected to be adequate for both internal and external forces and disturbances propagating to the patient because it depends mainly on isolating the disturbances rather than damping them.

2. Design of the isolation pad

The main design of this medical vibration isolation pad is based on dividing the whole pad into hexagons as a honeycomb as shown in Figure 1. All hexagons are attached to each other by a rubber sheet to allow flexible vertical movement of each hexagon separately in keeping them attached horizontally. This honeycomb configuration allows for decoupling motions and the decentralized control of each hexagon and reduces the influence of the transverse motion. The suggested model considers that the hexagons are completely separated from each other in terms of the vertical pumping mode motion which leads to simplifying the control technique and using a Single Input Single Output (SISO) method. Any side to side contact between the hexagons leads to improvements in the passive isolation authority as the hexagons will be covered by an elastomeric material with a significant passive damping content. One of the drawbacks of this design is the high cost because the piezoelectric actuators and sensors are expensive. According to the existence of high static force piezoelectric actuators, the number of actuators can be reduced in the pad to reduce the cost. Reducing the number of actuators will be accompanied by increasing the area of every hexagon supported by the actuator. Increasing the area of the hexagon reduces the frequency of the tilting and lateral vibration modes, getting them close to the vicinity of the first bounce

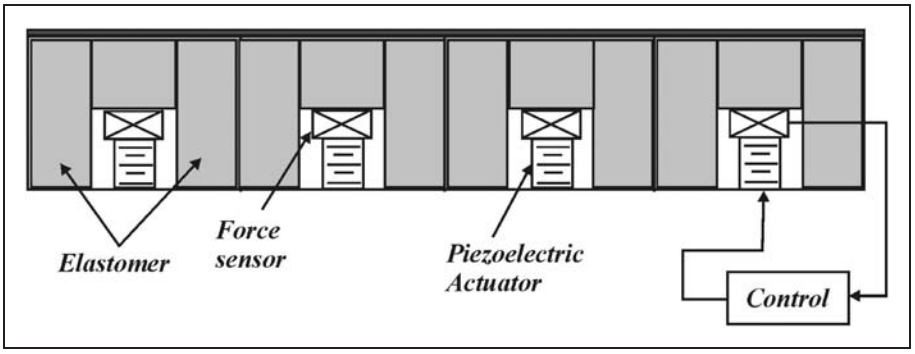

Figure 2. Active struts installation and control technique.

mode. As these modes are normal to the piezoelectric actuator and collocated sensor, they will be neither observable by the sensor nor controllable by the actuator. In this case, the only way to control these modes will be to add new lateral actuators in each hexagon, which is more complicated and more expensive than the proposed solution. On the other hand, there will be high coupling between these modes that leads to losing the benefit of the SISO system and requiring more complicated Multiple Input Multiple Output (MIMO) control techniques.

The cross-sectional view of the pad in Figure 2 shows the configuration and installation of the active struts inside the pad. Each active strut consists of a piezoelectric linear actuator in collocation with a piezoelectric force sensor, this active strut is mounted in a series with a soft rubber to reduce the corner frequency of the isolator. The active mounting will be installed in parallel with a rubber elastomer to help in the static stability of the system. The suggested control technique is based on using a feedback loop with a simple integrator. The system requires adding a high-pass filter at low frequency to avoid the propagation of wandering disturbance signals at low frequency and another low-pass filter to prevent the system from the deteriorating high frequency perturbations.

3. Modeling of the isolation pad

The pad is divided into separated hexagons where each hexagon envelopes a circle with a diameter of 150 mm and a height of 100 mm, as shown in Figure 3.

Each hexagon is supported by an active strut in the middle. The active strut consists of a piezoelectric actuator and a piezoelectric force sensor. The strut is supposed to carry and control vertical loads only, which enables the different hexagons to behave separately in a decoupled and a decentralized manner. Figure 4 shows a schematic representation of the active strut used for

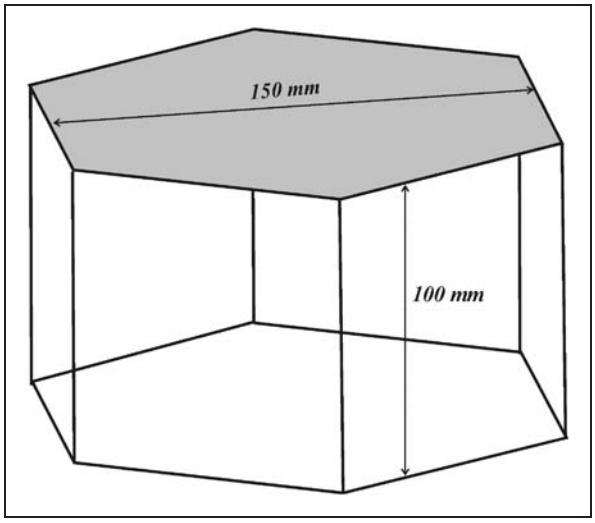

Figure 3. Wire Computer Aided Design of a hexagon.

active isolation where M represents the part of the patient's mass (load) carried by this part (hexagon) of the pad, m stands for the mass of pad's rubber intermediate between the patient and the actuator, k and c are the stiffness and damping coefficients of the rubber material used to fabricate the pad, respectively. The extension stroke of the piezoelectric actuator is denoted by δ where the stiffness of the preloading spring of the actuator is denoted by k_a. F represents the reading of the force sensor which is in reality the total force transmitted through the active strut to the intermediate rubber of the pad. The three displacements x, x_m and x_d stand, respectively, for the displacement of the patient, the displacement of the intermediate rubber and the displacement of the ground caused by the disturbance. The model represented schematically in Figure 4 can be expressed in the block diagram shown in Figure 5.

Taking into account the schematic representation in Figure 4 and the block diagram in Figure 5 with the

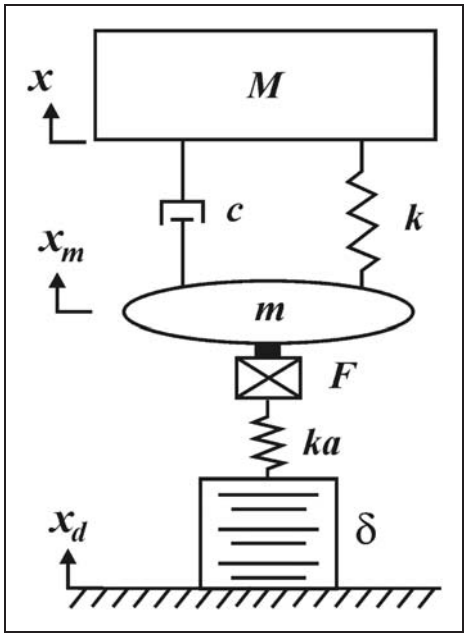

Figure 4. Schematic representation of the active isolation system.

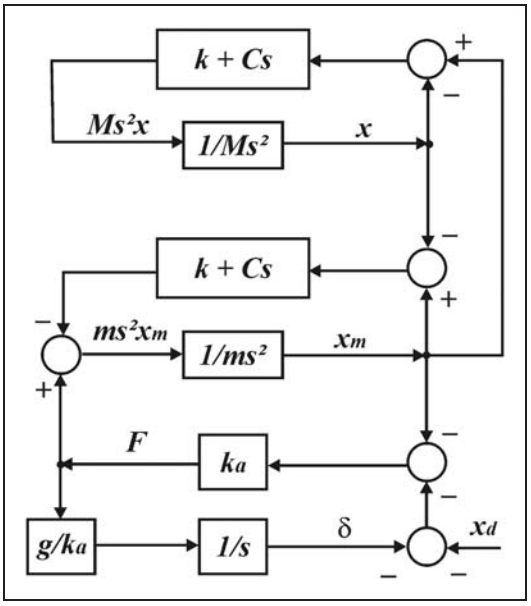

Figure 5. Block diagram for the system.

specified notations, the system can be represented mathematically by two second order linear differential equations. The rubber mass of the pad is mounted on the active strut and loaded by the patient can be governed by the equation:

$$m\ddot{x}_m + k(x_m - x) + c(\dot{x}_m - \dot{x}) - k_a(x_d - x_m) = k_a\delta \quad (1)$$

The human patient mounted on top of the elastomeric rubber can be represented by the following governing equation:

$$M\ddot{x} + k(x - x_m) + c(\dot{x} - \dot{x}_m) = 0 \quad (2)$$

Equations (1) and (2) can also be represented in matrix form as follows:

$$\begin{bmatrix} m & 0 \\ 0 & M \end{bmatrix} \begin{Bmatrix} \ddot{x}_m \\ \ddot{x} \end{Bmatrix} + c \begin{bmatrix} 1 & -1 \\ -1 & 1 \end{bmatrix} \begin{Bmatrix} \dot{x}_m \\ \dot{x} \end{Bmatrix} + k \begin{bmatrix} 1 + \frac{k_a}{k} & -1 \\ -1 & 1 \end{bmatrix} \begin{Bmatrix} x_m \\ x \end{Bmatrix} = k_a \begin{bmatrix} 1 & 1 \\ 0 & 0 \end{bmatrix} \begin{Bmatrix} x_d \\ \delta \end{Bmatrix} \quad (3)$$

The output equation that represents the reading of the force sensor reads:

$$F = k_a(x_d - x_m + \delta) \quad (4)$$

It is discussed deeply in Abu Hanieh (2009), Preumont (2002) and Preumont et al. (2002) that the IFF compensator ensures high stability and robustness for similar control systems. The controller is built by applying the IFF control technique on the system. The signal measured by the force sensor is integrated, multiplied by a gain $\boldsymbol{g}$ and fed back to the actuator. The required actuator's deflection $\boldsymbol{\delta}$ to overcome the exerted motion can be estimated from the following equation in Laplace form:

$$\delta = -\frac{g}{k_a}\frac{1}{s}F \quad (5)$$

Or

$$\delta = -\frac{g}{k_a}\frac{1}{s}k_a(x_d - x_m + \delta) \quad (6)$$

Manipulating this equation leads to a direct relationship between the deflection of the actuator and the relative displacement of the rubber motion to the ground motion as a function of the controller gain $\boldsymbol{g}$ which reads:

$$\delta = -\frac{g}{s+g}(x_m - x_d) \quad (7)$$

A low-pass filter can be added to the system at high frequency to cut-off the high frequency undesirable disturbances and to increase the high frequency attenuation. On the other hand, a high-pass filter can be added to the system at low frequency to prevent the system from low frequency signals propagating into the system and deteriorating the stability. This high-pass filter can help in the low frequency rigidity too, but it leads to

limitations in control authority where the system becomes conditionally stable. The other solution is to use a passive elastomer that helps in carrying the static loads, but this will reduce the high frequency attenuation from -40 dB/decade to -20 dB/decade due to increasing the order of the numerator of the transfer function. This attenuation decrease is solved by the low-pass filter as mentioned before.

4. Simulation results

4.1. Finite Element Model (FEM)

An FEM for a single hexagonal cell of the system without actuator has been simulated using CATIA software.

The dynamic analysis has been performed by applying the same boundary conditions as the static analysis. The first vibration mode was found to be at 3.5 Hz with a pumping up and down vertical modal shape as shown in Figure 6. This is considered the most dangerous mode on which the control has the highest authority, as there is only one actuator in the vertical orientation. Nevertheless, the high frequency modes are influenced by the control too.

The static analysis was taken by fixing the boundary walls of the hexagonal cell and applying a distributed force equal to half the weight of a normal human being (50 kg) on the surface. The static analysis showed that the maximum displacement is expected to be in the center of the hexagon with a static magnitude of 28.4 mm, as shown in Figure 7. This also gives an indication of the maximum strain energy fraction that gives the best location for the control actuator placement.

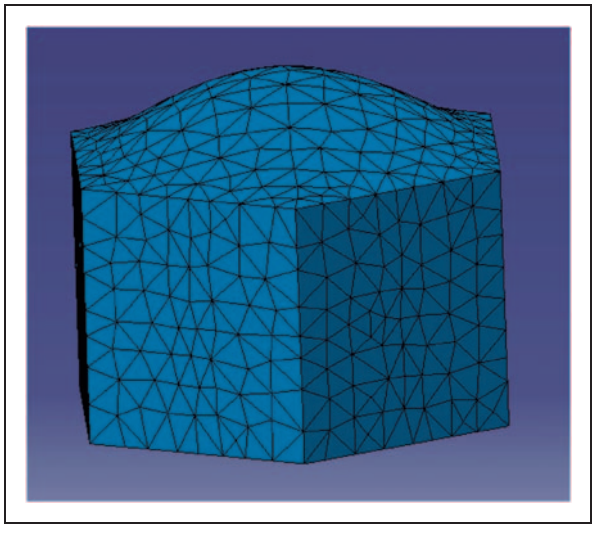

Figure 6. First vibration mode from dynamic Finite Element Model.

On the other hand, the stress analysis in Figure 8 shows that the maximum stress was 33.4 kPa at the edges of the hexagon due to the stretch that occurs to the rubber and tissue when loaded in static conditions. Stress analysis shows that the maximum static force required to withstand the load will not exceed 700 Newton in the worst case which is in the accepted range for newly designed amplified piezoelectric actuators. Remember that the weight of the patient has been distributed on two hexagons only, while in reality it is distributed more.

4.2. MATLAB Simulation

The isolation pad was modeled and simulated using Matlab-Simulink software. The system is considered

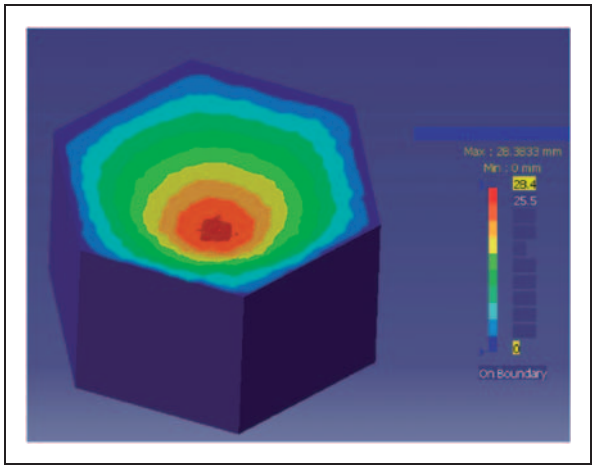

Figure 7. Maximum displacement from static Finite Element Model.

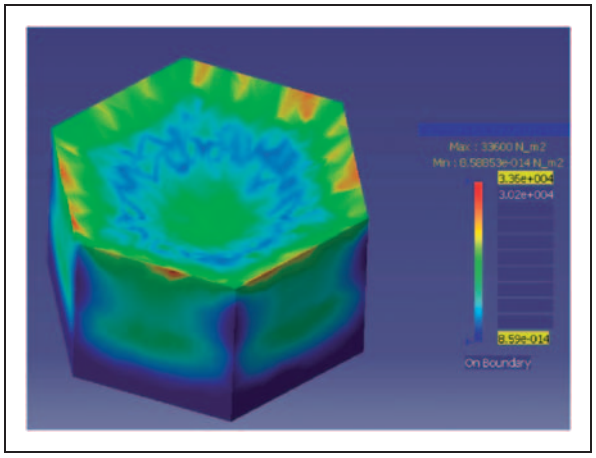

Figure 8. Maximum stress from static Finite Element Model.

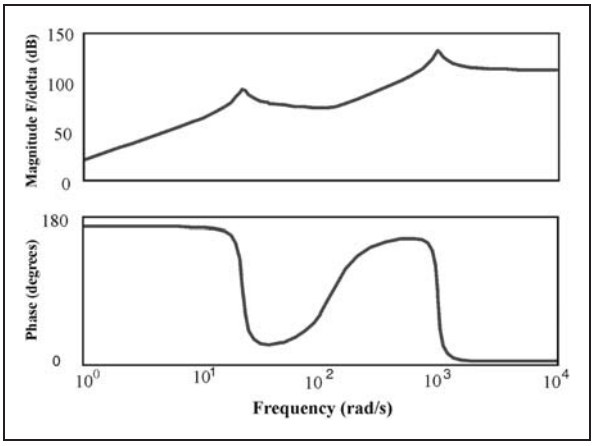

Figure 9. System Frequency Response Function (F/δ).

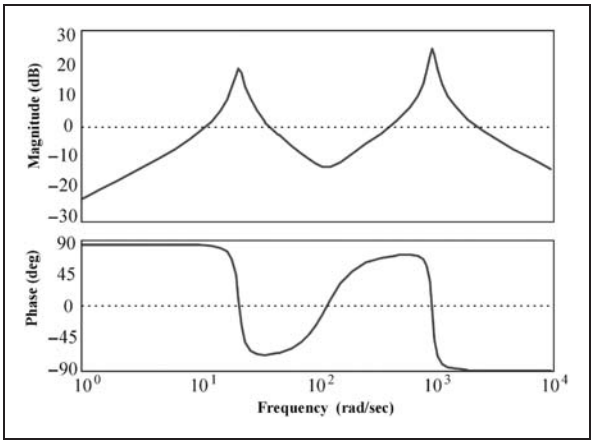

Figure 10. Open-loop Frequency Response Function (F/δ) with controller.

as a two-stage suspension where the first stage consists of a piezoelectric actuator, force sensor and a light mass representing the rubber of the pad. The second stage represents the patient's mass mounted on top of the stiffness and damping of the rubber as shown in Figure 4. Figure 9 shows the Frequency Response Function (FRF) of the system between the actuator displacement δ and the force sensor reading F. This FRF shows the natural frequencies of the system that represent the vibration modes, with the first mode at 21 rad/s (3.5 Hz) and the second mode at 1000 rad/s (161 Hz). The first mode is the most dangerous and represents the vertical vibration that deteriorates the patient's body influenced by the propagating disturbance coming from the ground and the magnet through the active system. The second mode, at high frequency, represents the vibration mode of the stiff mount calculated by the mass of the load and the stiffness of the piezoelectric actuator. The open-loop transfer function with the controller (integrator) connected in series is depicted in Figure 10. A simple check for stability of the system on the Bode plot shown in Figure 10 reveals that the phase margin reaches up to 90 degrees, which proves very high stability. Another check for the stability of this control technique can be taken from the root locus demonstrated in Figure 11. The root locus proves that closing the feedback loop with the integrator as a controller leads to unconditional stability. Figure 12 states the transmissibility FRF between the displacement of the ground coming from the external disturbance and the displacement of the patient without controller (dashed line) and with applying IFF controller (solid line). This figure shows that the proposed controller has a high performance and influence on the transmitted vibrations by reducing the overshoot peaks in the vicinity of the natural frequencies of the system without reducing the roll-off at high frequency.

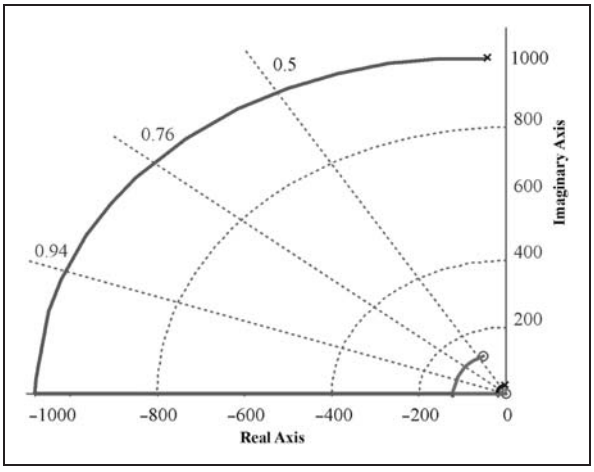

Figure 11. Root Locus diagram.

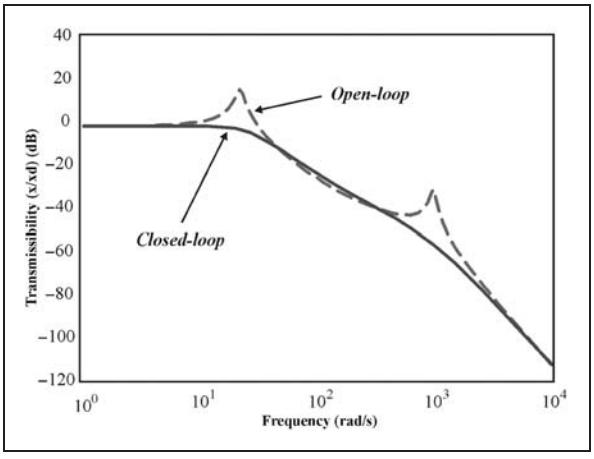

Figure 12. Transmissibility Frequency Response Function between the ground displacement and the patient's displacement.

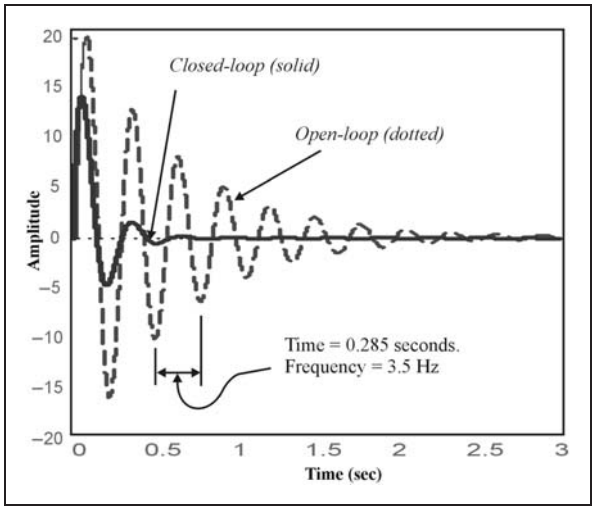

Figure 13. Time response for the displacement x without control (dotted line) and with applying Integral Force Feedback control (solid line).

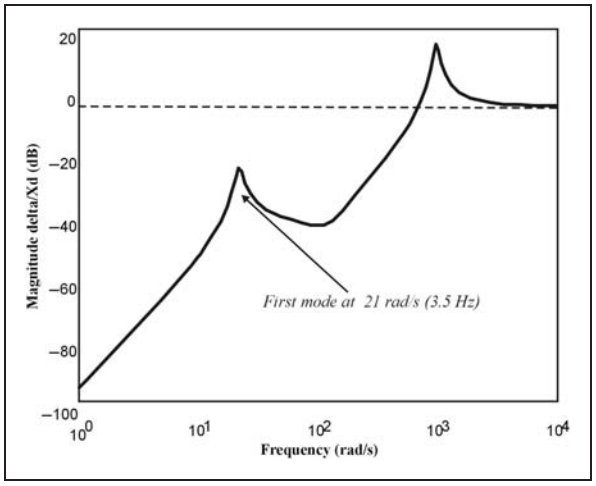

Figure 14. Transfer function in frequency domain between the disturbance x_d and the deflection of the actuator δ.

Figure 13 shows the transient response in time domain for the displacement of the patient's body x as influenced by the disturbance source x_d once without control (dotted line) and another time with applying the IFF controller (solid line) in the vicinity of the first vibration resonance at 3.5 Hz. Using the IFF control technique leads to unconditional stability that can be limited and turned to conditional stability if a high-pass filter is used at low frequency. It is clear that the time response is significantly improved where the system is settled down much earlier with control. The influence of the disturbance source x_d on the deflection of the piezoelectric actuator δ is depicted in Figure 14. It is evident from this FRF that the deflection is minimized at low frequency. In the vicinity of the first vibration mode it does not exceed -20 dB where the stroke required from the actuator equals to 10% of the disturbance displacement. This proves the possibility of using piezoelectric actuators with relatively low strokes. The required stroke of the actuator relative to disturbance increases with frequency, which can cause limitation at high frequencies, but this is not expected to cause a major problem because the high frequency modes are not drastic. On the other hand, the disturbance amplitude decreases significantly at high frequency. Reminding that the FRF in the figure shows the ratio between the disturbance and the deflection, it can be said that the required actuator's stroke is still reasonable. Figure 14 also gives an indication of the force required from the actuator to overcome the disturbance, because the force of the piezoelectric actuator can be calculated through multiplying the deflection by the stiffness ($F_a = k_a\ \delta$).

5. Conclusions

The foregoing research tackled the influence of vibrations induced by the MRI on the patient and imaging process. A glimpse of the previous efforts of other research groups has been discussed in brief showing the importance of the topic. The desired system has been modeled using two stage vibration isolation with a piezoelectric actuator and soft intermediate passive mount. The simplicity of the system leads to the simplicity of the controller. A simple integrator was applied to control the system where high authority and robustness were guaranteed. The analytical model was simulated using Matlab-Simulink software while the FEM was simulated using Catia software. A good match is found between the two models focusing on the first pumping vibration mode because there is a wide frequency gap between the first and the second mode.

So far, the system has been verified by modeling and simulation only. In the near future, the system will be presented by an experimental prototype and some practical results will be obtained and compared to the theoretical and analytical work done in this paper. After testing one cell, a complete pad set-up will be tested and studied to check the possibility of controlling each cell separately and to test the decoupling idea stated before.

Funding

This research received no specific grant from any funding agency in the public, commercial, or not-for-profit sectors.

References

Abu Hanieh A (2008) Vibration isolation of hand-held tools to prevent hand-arm vibration syndrome. *International*

Review of Mechanical Engineering (IREME) 2(2): 290–295.

Abu Hanieh A (2009) *Active Isolation and Control of Vibrations, via Stewart Platform*. Saarbriicken, Germany: VDM Verlag.

Evans J and Philbin M (2000) The acoustic environment of hospital nurseries: facility and operations planning for quiet hospital nurseries. *Journal of Perinatology* 20: 105–112.

Evans J (2003) Structural floor design for a magnetic resonance system (MRI) utilizing resonant frequency detuning and dynamic analysis. In *Proceedings of the Tenth International Congress on Sound and Vibration*, Stockholm, Sweden, July 7–10, p.112.

Evans J (2004) Analysis of ambient sound levels and simulated demolition/construction impact noise. Stein-Cox Group, Architects and Phoenix Children's Hospital. *Journal of Acoustics* Rpt 2420–1.

Hao K (2008) Investigation of elestomeric pad attenuation of hand-transmitted vibration. Master Thesis, Universiti Sains Malaysia.

Jaensch M, Young I, Besant C, Atkins A and Lamperth M (2007) Development of the technical capabilities needed to build and position a prepolarization coil for a magnetic resonance imaging magnet. In *Proceedings of the Institution of Mechanical Engineers, Part H: Journal of Engineering in Medicine* 221(2): 185–194.

Le Letty R and Claeyssen F (1998) Piezoactuators and piezo motors for high strokes/precise positioning applications. In *Proceedings of Actuator 98 Conference,* Bremen, Germany, June 17–19, pp. 170–173.

Mechefske C, Yao G and Wang F (2004) Vibration and acoustic noise characterization of a gradient coil insert in a 4 T MRI. *Journal of Vibration and Control* 10: 861.

Nelson P (1991) An active vibration isolation system for inertial reference and precision measurement. *Review of Scientific Instruments, American Institute of Physics* 62(9): 2069–2075.

Preumont A (2002) *Vibration Control of Active Structures*, 2nd edn. Dordrecht, The Netherlands: Kluwer Academic Publishers, pp. 116–121.

Preumont A, Francois A, Bossens F and Abu Hanieh A (2002) Force feedback vs. acceleration feedback in active vibration isolation. *Journal of Sound and Vibration* 257(4): 605–613.

Schubert D, Beard A, Shedd S, Earles M and Von Flotow A (1994) Stiff actuator active vibration isolation system. *US Patent 5,823,307*.

Standlee K and Begin J (2003) The MRI - a noise source of concern in the healthcare industry. *Journal of Acoustical Society of America* 114(4): p. 2327.

Wakui S (2002) Active vibration isolation device and its control method. *US Patent 6,378,672 B1*.